Estonian Journal of Engineering, 2010, **16**, 3, 187–210 doi: 10.3176/eng.2010.3.01

The use of high-resolution bathymetry for circulation modelling in the Gulf of Finland

Oleg Andrejev[a], Alexander Sokolov[b], Tarmo Soomere[c], Rolf Värv[c] and Bert Viikmäe[c]

[a] Finnish Environment Institute, P.O. Box 140, FI-00251, Helsinki, Finland
[b] Baltic Nest Institute, Stockholm Resilience Centre, Stockholm University, SE-10691 Stockholm, Sweden
[c] Institute of Cybernetics at Tallinn University of Technology, Akadeemia tee 21, 12618 Tallinn, Estonia; soomere@cs.ioc.ee

Received 14 June 2010, in revised form 5 July 2010

Abstract. We present preliminary results of the extension of the OAAS circulation model to a high-resolution bathymetry with a finest resolution of 0.25 nautical miles in the Gulf of Finland, the Baltic Sea. The models with a resolution of 1 mile or finer are capable of resolving typical mesoscale eddies in this basin where the internal Rossby radius is usually 2–4 km. An increase in the model resolution from 1 to 0.5 NM leads to a clear improvement of the representation of the key hydrophysical fields. A further increase in the resolution to 0.25 NM has a lesser impact on hydrophysical fields, but may lead to some changes in the instantaneous patterns of currents. The parameterization of the spreading effect of sub-grid-scale turbulence on the trajectories of initially closely located drifters is realized by means of accounting for the largely rotational character of the dynamics in this basin. The modelled average spreading rate for initially closely located particles for 1991 was 2 mm/s.

Key words: circulation modelling, Gulf of Finland, Baltic Sea, bathymetry, sub-grid turbulence, turbulent spreading.

1. INTRODUCTION

Recent research [1] has shown that the best existing 3D scientific circulation models are able to replicate the major features of the hydrophysical fields of the Gulf of Finland and to resolve the most important features of the dynamics of currents in this basin. For example, the hindcast mean temperatures differ from observations by less than 1–2 °C and the mean error in salinity is less than 1‰. While there are some deviations in the modelled variables from the measured

ones in single model simulations, ensemble-averaged results show no systematic over- or underestimation. Most of the remaining difficulties that will increase the accuracy of simulations of the hydrography if solved, are connected with problems in adequately representing the dynamics of the mixed layer. The loss of accuracy is most notable in the simulation of the depth and the sharpness of the corresponding thermo- and haloclines. Despite the application of sophisticated turbulent closure schemes and different schemes for vertical mixing, none of the models, analysed in [1], were able to accurately replicate the vertical profiles of temperature and salinity.

Another bottleneck is the low accuracy of the reproduction of the patterns of currents. An adequate picture of mesoscale dynamics is especially important for applications such as the forecast of drift of various substances that rely on the properties of instantaneous currents. The prediction of surface drift is a very challenging task, even in sea areas with relatively simple internal dynamics because even small errors in the estimates of current patterns can drastically change the calculated particle trajectories [2]. Several authors claim that as yet deterministic methods to adequately reproduce the floating object drift are missing [3]. As an alternative, recent attempts to estimate the drift and transport patterns in sea areas with complicated dynamics [4,5] use statistical analysis of large pools of simulations. Instead of aiming at an exact reconstruction or forecast of single trajectories of floating objects, they rely on the assumption that the statistics of the drift patterns (consequently, statistics of currents and the related transport) are correctly captured by the underlying simulation model.

The key purpose of this paper is to increase the accuracy of simulation of drift patterns in the Gulf of Finland by means of a considerable increase in the effective resolution of the bathymetric information and accounting for the mostly rotational character of currents in this water body in the modelling of sub-grid-scale effects.

In order to replicate the statistics of mesoscale effects, the relevant numerical scheme has to resolve the majority of dynamic features with typical scales about the internal Rossby radius of deformation R_1. In other words, the horizontal grid step Δy has to be considerably smaller than R_1. Usually it is considered necessary to use $\Delta y \le 0.5R_1$ [6,7]. There has been rapid progress towards increasing the spatial resolution of the Baltic Sea circulation models. Mesoscale-resolving models are now widely used, for example, in the Baltic Proper [8,9], where usually $R_1 > 10$ km and a grid step of 2 NM resolves most of the mesoscale effects.

The situation is less satisfactory in the Gulf of Finland where R_1 is very small (Fig. 1), usually 2–4 km [10]. Therefore it is not surprising that the success of the modelling efforts, especially in this basin, strongly depends on the horizontal and vertical resolution in use. Several larger mesoscale features, such as fronts at the entrance to this gulf, large coastal upwellings and a part of their filaments can be reasonably reproduced for this environment with the use of grid size of 2–3 NM [1,11]. Such models, however, may overlook some of the dynamic features

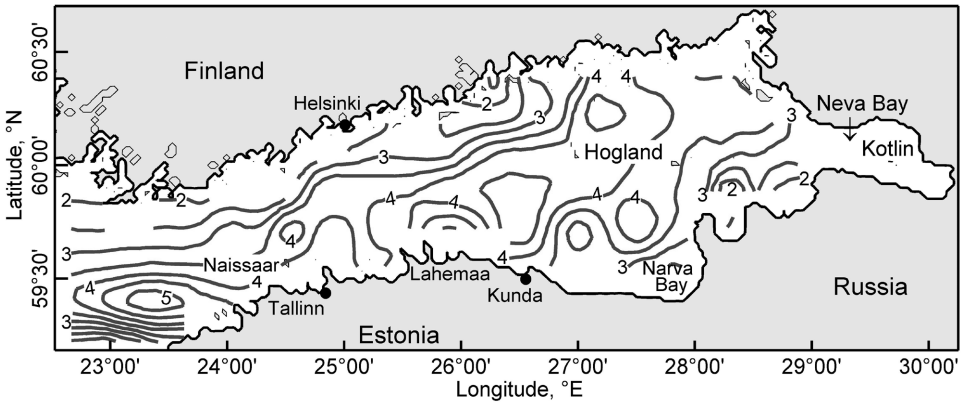

Fig. 1. Spatial variation of the internal Rossby radius (km) in the Gulf of Finland [10]. The coastline is drawn based on the depth data from [14].

in the Gulf of Finland where resolving the dynamics of mesoscale eddies (at least in terms of their statistics) requires the use of a horizontal resolution down to 1 NM or even less. This requirement should be satisfied for all wind conditions. This is because the instantaneous field of currents is an integral reaction of water masses to a variety of forcing factors distributed over large sea areas. It is a highly nontrivial, non-stationary system even for practically stationary wind conditions that do not necessarily follow the patterns of wind properties over particular sea areas [12,13].

An intriguing feature established in [1] is that the existing models were generally more accurate in the western gulf than in the east although uncertainties connected with the impact of the open Baltic Sea dynamics to the local features should be larger in the west. Two potential reasons behind this feature were discussed. First, insufficient vertical resolution may lead to generic difficulties in simulating the hydrodynamics of the eastern gulf because of the steeper gradients in salinity due to the large freshwater discharge. Second, the resolution of the bottom topography was insufficient to describe many of the small-scale features in the shallower eastern gulf.

Most of the models in use rely on the bathymetric information from [14] with a spatial resolution of about 1 NM. This data set (optionally adjusted for specific purposes by means of removing almost closed bays etc.) is used in many contemporary circulation and wave models [1,12,15–22]. There are several attempts to increase the formal resolution of this dataset to 0.5 NM by means of interpolation of the existing information [19,20,22]. Doing so obviously leads to a better resolution of mesoscale effects in areas with a relatively plane bottom, and consequently to a better match of the simulated hydrodynamic and hydrophysical fields with reality. Nevertheless, much of the dynamics of the Gulf of Finland is apparently significantly affected by the local topography. Its role is the largest in the northern part of the gulf where the bottom is in places extremely rugged and the geometry of the archipelago and the Finnish coastline is extremely complex.

Also, inadequate representation of the cross-section of the deep-water passages in the narrowest part of the gulf (combined with the insufficient vertical resolution of the models) may adversely affect the accuracy of the reproduction of hydrophysical properties in the western part of the gulf. In order to properly account for these features, additional information must be incorporated into the models in a consistent manner.

A systematic increase in the spatial resolution and overall accuracy of the circulation models towards capturing (the statistics of) the drift of floating objects is of key importance from the viewpoint of attempts to detect semi-persistent patterns of currents and areas of reduced risk in the Gulf of Finland with the goal of identification of an optimum fairway in this basin in terms of environmental considerations [4,5].

In this paper, we describe a new gridded bathymetric data set with a resolution of 0.5 NM (0.25 NM in areas where high-resolution maps are available) for the Gulf of Finland. The use of such data allows for a consistent increase in both the horizontal and vertical resolution of the circulation model for this basin along with certain changes in the model physics. The first runs with a horizontal resolution of 1 NM, based on the new data, reveal realistic behaviour of the vertical structure of the hydrophysical fields whereas the runs with a resolution of 0.5 NM demonstrate the level of complexity and number of the details of the simulated fields similar to those observed from satellites. Finally, we introduce a new method (mirroring the prevalence of circularly polarized motions in the Gulf of Finland) for the simulation of the effect of sub-grid turbulence on the spreading of initially close trajectories of floating objects.

2. HIGH RESOLUTION BATHYMETRY FOR THE GULF OF FINLAND

The most frequently used bathymetry for the Baltic Sea, including the Gulf of Finland, was derived a decade ago [14,23]. This publicly available data set gives the average water depth for rectangles of 2′ along longitudes and 1′ along latitudes. Equivalently, it has a spatial resolution of about 1 NM at latitude of the Gulf of Finland. As this data set has not been specifically tuned for hydrodynamic simulations, different users have used different adjustments in order to achieve the best performance of their models.

There have been a few attempts to construct a bathymetry for the Gulf of Finland at a higher resolution. For example, a bathymetry with a step of 0.5 NM was constructed in [19,20] by means of straightforward interpolation of the data set of [14]. Recently, the Danish Meteorological Institute has launched a semi-operational circulation and oil spill model for the Gulf of Finland at 0.5 NM resolution, also using interpolation (J. Murawsky, pers. comm., 2010). Doing this obviously allows for a better match of the model resolution with the above requirements arising from the size of the Rossby radius, and leads to excellent reproduction of several interesting dynamic features [19,20,22]. However, the

problems described above, with the potential distortions of the results caused by insufficient underlying bathymetric information, still persist.

A sustainable way forward is the physical improvement of the bathymetric information. Attempts in this direction, based on public marine charts [17,24–28], have been made within the framework of multi-nested modelling of currents and wave fields for small coastal areas. These attempts are the most systematic for the eastern part of the Gulf of Finland where the resolution of 1 NM is obviously insufficient [29]. A significant improvement in the representation of the bottom topography for the easternmost Gulf of Finland (including Neva Bay) has been recently implemented in [30].

In order to reach a more consistent improvement of the bathymetry, the water depths to the east from longitude 23°30′ in the Gulf of Finland were gridded with a spatial resolution of 0.25–0.5′ along latitudes and 0.5′–1′ along longitudes, that is, with an effective spatial resolution of about 470–930 m. The basic information was extracted from public marine charts that exist at 1 : 50 000 scale along the coasts of Finland and Estonia. These maps usually contain at least one depth mark for almost every grid cell with dimensions of about 470 × 470 m. A bilinear interpolation combined with information extracted from the position of isobaths and a rough estimate of the depth gradient at adjacent cells was used to estimate the depth at a few cells where no direct information was available. The resulting grid was manually adjusted in the coastal and archipelago areas in order to ensure the presence of relatively narrow straits in the grid geometry by means of adding, when necessary, a sea point to the grid, and to mimic the impact of the presence of clusters of small islands to the circulation patterns by means of inserting dry land in such areas. In areas with a relatively rugged bottom, the values for the depth at certain grid cells were adjusted so that the position of the resulting isobaths matched those given on the original maps. Finally, a model grid with a uniform spatial resolution of 0.5′ along latitudes and 1′ along longitudes was constructed from this data set. The resulting 0.5 NM grid also needed some manual adjustment in order to represent several features of the Finnish archipelago. Another grid with a formal resolution of 0.25 × 0.5′ over the entire Gulf of Finland was created from this set by means of linear interpolation of the depths in four sub-cells of the data with a resolution of 0.5 × 0.1′.

It is not surprising that the properties of the resulting grids match better the classical estimates for the average depth of the Gulf of Finland (37–38 m according to different authors) than that constructed in [14] (Table 1). The formal mean depth of the basin at 0.5 and 1 NM resolution slightly exceeds that calculated at 0.25 NM resolution. The small difference probably reflects a relatively large number of neglected coastal sea points (representing, for example, narrow bays deeply cut into land or passages in the archipelago that are present in the 0.25 NM grid) in the 0.5 NM and coarser resolution.

The resulting grid (Fig. 2) adequately reproduces the basic features of the sea bottom in the southern and south-eastern parts of the Gulf of Finland. It is, however, not capable of reflecting the entire variability of the Finnish archipelago and

Table 1. Parameters of different versions of the bathymetry of the Gulf of Finland and the associated model runs

	Resolution, NM			
	0.25	0.5	1	1 [14]
N	127 622	31 838	8 810	8 810
$\bar{H}$, m	38.2	38.4	38.4	35.0
σ, m	23.6	23.6	23.6	22.0
B, m	0.0	0.2	0.2	–3.2
Vertical layers	105	105	92	–
Δt, s	72	144	180	–

N is the number of sea points, H_i is the depth in a particular grid cell, $\bar{H} = \frac{1}{N}\sum_{i=1}^{N} H_i$ is the mean depth, the root-mean-square deviation is calculated as $(N-1)\sigma^2 = \sum_{i=1}^{N}(H_i - \bar{H})^2$, $B = \bar{H} - \bar{H}_{0.25}$ is bias with respect to the mean depth according to the bathymetry with a 0.25 NM resolution and Δt is time step.

the northern coast of the gulf where many objects still remain in the sub-grid scale and the gridded information substantially smoothes the reality. There are some shortcomings of this grid, connected with an insufficient resolution of depth information in the relatively deep central part of the gulf and in the eastern part of the gulf, for which public high-resolution maps are not available. These areas (in which the actual spatial resolution of the gridded information is of the order of 1 km) are visible in the map as regions with unreasonably smooth seabed compared to the adjacent regions. The bathymetry of the sea area between Tallinn and Helsinki in three resolutions is shown in Fig. 3. The general impression from Fig. 3 is that a shift from a 1 NM grid to a 0.5 NM grid should result in a considerable improvement in the depiction of the structure of the seabed while the further implementation of a 0.25 NM grid might be important for coastal areas.

3. CIRCULATION MODEL

The circulation simulations described in this paper are based on the updated version of the numerical model OAAS (Oleg Andrejev and Aleksandr Sokolov) [31,32], which was developed specifically for use in basins with complicated bathymetry and hydrography, such as the Gulf of Finland. The model follows the logic of the Princeton Ocean Model [33] and is based on the system of primitive equations of horizontal momentum balance, continuity equation, equation of state, hydrostatic equation, and equations for transport of heat and salt. The model employs standard simplifications used in large-scale circulation modelling such as the assumption of incompressibility of the flow (which only filters out

acoustic waves that are negligible for circulation) and the Boussinesq hydrostatic approximation in which the vertical density variations are ignored in the equations of horizontal momentum balance and are accounted for only in the buoyancy terms. The system thus consists of the equations of motion for the horizontal velocity components (u, v) in the x and y directions

$$\frac{\partial u}{\partial t} + u\frac{\partial u}{\partial x} + v\frac{\partial u}{\partial y} + w\frac{\partial u}{\partial z} = fv - \frac{1}{\rho_0}\frac{\partial p}{\partial x} + \mu\Delta u + \frac{\partial}{\partial z}\left(\vartheta\frac{\partial u}{\partial z}\right), \tag{1}$$

$$\frac{\partial v}{\partial t} + u\frac{\partial v}{\partial x} + v\frac{\partial v}{\partial y} + w\frac{\partial v}{\partial z} = -fu - \frac{1}{\rho_0}\frac{\partial p}{\partial y} + \mu\Delta v + \frac{\partial}{\partial z}\left(\vartheta\frac{\partial v}{\partial z}\right), \tag{2}$$

the Boussinesq approximation and the continuity equation for incompressible flows:

$$\frac{\partial \rho}{\partial z} = pg, \qquad \frac{\partial u}{\partial x} + \frac{\partial v}{\partial y} + \frac{\partial w}{\partial z} = 0. \tag{3}$$

Here x increases eastwards, y northwards and z downwards, the vertical velocity is denoted by w, Coriolis parameter by f, pressure by p, ρ_0 is the reference density, Δ is the horizontal Laplacian operator and g is the acceleration due to gravity. As usual, the effect of local, sub-grid-scale turbulence is separated into two parts to some extent mirroring the difference of the horizontal and vertical scales in the ocean. Different from the previous model versions, the horizontal turbulence is now parameterized with the use of the classical Smagorinsky scheme [34] while for the vertical small-scale motions the so-called Prandtl–Obukhov formula [35] is employed. The kinematic eddy diffusivity coefficients in the horizontal and vertical directions are μ and ϑ, respectively.

The equation of state $\rho = \rho(T, S)$ is used in the completely implicit formulation, derived specifically for the Baltic Sea conditions [36]. The equation for the transport of scalar quantities (salt S and heat $\rho C_p T$; here A stands for either of them) is as follows:

$$\frac{\partial A}{\partial t} + \frac{\partial uA}{\partial x} + \frac{\partial vA}{\partial y} + \frac{\partial wA}{\partial z} = \mu_A \Delta A + \frac{\partial}{\partial z}\left(\vartheta_A \frac{\partial A}{\partial z}\right) + F_A. \tag{4}$$

Here, C_p is the specific heat of water, T is the temperature, and F_A stands for the sources or sinks of the relevant quantities within the model domain.

The model is implemented in time-dependent, free-surface conditions and adequately accounts for all baroclinic effects. The north-south variation of the Coriolis acceleration (which is crucial for properly resolving the mesoscale phenomena) is fully accounted for by means of using the exact value of the Coriolis parameter f for each latitude. Notice that the equations are solved in rectangular coordinates whereas the bathymetry is presented in spherical

coordinates. Doing so is acceptable in the Gulf of Finland conditions because this water body is relatively narrow and elongated in the east-west direction. A rough estimate for the associated error caused by this approximation is the relative difference between the grid cells with the maximum and minimum areas, which is about 3% and thus much less than the typical uncertainty of the bathymetry. The simulations performed with the use of the new bathymetry with resolutions of 1, 0.5 and 0.25 NM (especially with the use of the 0.5 and 0.25 NM model grids where the vertical resolution has been substantially increased: the model comprised 105 layers) are, therefore, basically capable of the reproduction of all the 3D variability of hydrographic and kinematic parameters in the grid scale.

The model is forced by wind stress $\vec{\tau} = (\tau_x, \tau_y)$ and bottom friction enters as a boundary condition. For the sea-surface $z = -\varsigma(x, y, t)$ these are:

$$\vartheta \frac{\partial u}{\partial z} = \frac{-\tau_x}{\rho_0}, \quad \vartheta \frac{\partial v}{\partial z} = \frac{-\tau_y}{\rho_0}, \quad \vartheta_T \frac{\partial T}{\partial z} = -q_T, \quad \vartheta_S \frac{\partial S}{\partial z} = -q_S. \tag{5}$$

Here, pressure on the sea surface is set equal to the air pressure p_a, ς is the elevation of the free surface and q_T and q_S are the heat and salt fluxes, respectively. The kinematic boundary condition

$$w = \frac{\partial \varsigma}{\partial t} + u\frac{\partial \varsigma}{\partial x} + v\frac{\partial \varsigma}{\partial y} \tag{6}$$

signifies that a fluid particle at the surface remains there forever (as is typical for boundary problems for both circulation and wave motion). Over the entire sea-bed the no-slip (first type Dirichlet) condition is applied for all velocity components. As usual, the sea-bed is assumed to be non-permeable also for the scalar properties such as temperature and salinity for which Neumann conditions are applied. Thus, the boundary conditions are:

$$u = v = w = 0, \quad \vartheta_T \frac{\partial T}{\partial z} = \vartheta_S \frac{\partial S}{\partial z} = 0 \quad \text{at} \quad z = H(x, y). \tag{7}$$

The wind stress components are taken in the form $\tau_{x,y} = \rho_a C_d \vec{W}_{x,y} |\vec{W}|$ [37], where $\vec{W}$ is the wind velocity and ρ_a is the density of air. Following [38], the drag coefficient C_d at the sea-surface is formulated as

$$C_d = 0.0012(0.066|\vec{W}| + 0.63). \tag{8}$$

The bottom stress is also expressed classically, in the form of a quadratic law [39] with the bottom drag coefficient $C_b = 0.0026$ [40].

Some important distinguishing features of the OAAS model from several other families of circulation models are in the details of the numerical scheme [31,32,41]. The use of the governing equations in the flux form ensures that a number of integral constraints [36] are maintained automatically. The finite-

difference method uses the Arakawa C-grid [42] and the method of splitting the time step [43]. All vertical derivatives and the bottom friction are treated implicitly.

The model uses the mode-splitting technique [44]: the 2D equation for the volume transport (the external mode) is obtained by vertical summation of the finite-difference approximations of the 3D momentum equations (internal modes). Before these equations can be solved, the sea-surface elevation must be calculated from the above volume transport equation and the vertically integrated continuity equation. The frictional stress at the bottom enters semi-implicitly into both modes and is based on the iteratively calculated bottom-layer velocity. These 2D and 3D equations are solved repeatedly until the maximum difference between the bottom velocities for subsequent iterations becomes smaller than a prescribed small threshold of 1 cm/s. An implicit alternating direction method is used for solving the volume transport equation [31,43]. This scheme allows the use of the same time step (in the present study 72–180 s depending on the resolution, see Table 1) for both the 2D and 3D elements of the model. The Gaussian elimination method (Thomas algorithm) makes it possible to rapidly solve these equations.

For test runs, the model was only run for the Gulf of Finland in a simpler, stand-alone version in which the vertical structure of the hydrophysical fields on the western boundary of the simulation area was accounted for but the heat flux and exchange of mass and momentum were ignored. In this model setup, so-called radiation conditions for both surface elevation [45,46] and for other variables, optionally with the sponge layer approach, were used.

For the experiments described below, we use the 3D structure of the salinity and temperature field and sea level information at the boundary with the Baltic Sea from long-term simulations performed with the Rossby Centre coupled ice-ocean model (RCO). This model has been developed using the version of the Ocean Circulation Climate Advanced Modelling (OCCAM) project of the Bryan-Cox-Sempner primitive equation ocean model with free surface. The RCO model contains parameterizations, important for the Baltic Sea (a two-equation turbulence closure scheme, open boundary conditions, and a sea-ice model), and is run with a horizontal resolution of 2 NM that is usually sufficient for eddy-resolving runs in the Baltic Proper [8,9]. In these cases, only the dynamics in the Gulf of Finland are simulated by the OAAS model in a high resolution. To smooth the potential impact of the difference in the resolution between the RCO and OAAS models, a so-called sponge layer of a width of 16 grid cells is defined as the zone where the lateral diffusivity coefficient increases towards the open boundary following a sine function.

The initial sea water temperature and salinity fields have been constructed using RCO data. At the start of the calculations, current velocities are set to zero while sea level deviation from the mean value is calculated using the so-called barometer solution in order to find equilibrium with atmospheric pressure. The typical spin-up time for the Gulf of Finland dynamics is from a few weeks to a

few months and thus, the first months of the runs have not been used in the analysis.

For meteorological forcing, we used the relevant fields downscaled from the ERA-40 database using a regional atmosphere model covering the entire Baltic Sea with a horizontal resolution of 12 NM (about 22 km) [47]. The meteorological fields contain surface pressure, temperature, wind speed components, total precipitation, snow depth, actual albedo, short and long wave radiation, evaporation, relative and specific humidity and total cloud cover with a temporal resolution of 3 h.

River discharge is prescribed based on the Bergström and Carlsson data set [48] in terms of monthly mean values for 1970–1990. The salinity of river water is set to zero and its temperature equal to the ambient sea water temperature at the river mouth. This approximation (equivalent to ignoring both salinity and heat flux from the rivers) is logical for the Baltic Sea conditions where both the river discharge and the difference in river and sea water temperatures in shallow river mouth areas are moderate. Note that there are applications where river water temperature is important and the relevant measurements have been used for circulation simulations [1].

The winters during the period of interest (1987–1992) were rather mild. In accordance to the information from the Finnish Ice Service (A. Seinä, pers. comm.) and according to the standard classification of ice-conditions, three of these winters were extremely mild, one was mild and only the winter of 1988 showed average conditions. Hence the Gulf of Finland was mostly free of ice, which permits us to assume that a simple parameterization can be used to describe ice formation and destruction. Even though no ice-drift mechanism is modelled, the effects of sea ice are taken into account as follows. For water temperatures below –0.2 °C, the wind stress is decreased by a factor of 10 in order to mimic the resulting tilt of the ice-covered surface. At 0 °C, the heat flux through the ice ceases as long as cooling conditions prevail. When the heat flux becomes positive in the early spring, it is decreased by the factor of four until sea water temperature reaches the value of +1 °C. This approach accounts for the loss of heat during ice melting.

4. HYDROGRAPHIC FIELDS

The performance of the OAAS model in a medium resolution (1 NM) grid, based on the data from [14], has been estimated in a number of earlier studies [1,12,13,15]. In particular, the difference in the results obtained with the OAAS model with resolutions of 1 and 2 NM have been extensively discussed [49]. For this reason, we only present here a few qualitative issues demonstrating how the model represents the basic hydrography and complexity of the dynamics of the Gulf of Finland.

Figures 4–6 demonstrate the potential of the high-resolution simulations for opening new horizons in the replication of the hydrophysical fields of the Gulf of

Finland. These images have been calculated with the use of the OAAS model with a spatial resolution of 1, 0.5 or 0.25 NM, constructed on the basis of the gridded depth information and the forcing in the Gulf of Finland eastwards from the longitude 23°30′E as described above. The boundary conditions (3D hydrographic fields along this longitude) have been extracted from the RCO model output.

Figure 4 shows that the OAAS model reproduces, as expected, the formation of an intermediate layer of relatively cold water in the Gulf of Finland during the winter and spring seasons (Fig. 5) [50]. This layer, when undisturbed by up/downwellings, lies below the layer of warmer (and somewhat less salty) water, and its thickness gradually increases in spring. Here, it starts from the depth of about 10 m and has a typical thickness of about 20 m. On top of it is a thin (3–6 m) layer of water that has been warmed during spring.

The calculated surface salinity field (Fig. 5) corresponds to an upwelling event of moderate magnitude along the Finnish coast. The upwelling brought to the surface water from the layer of 'old' relatively cold water. As a result, colder water with a comparatively large salinity is found to the north of the gulf axis between the Tallinn-Helsinki line and Suursaar (Hogland). An inflow of salty water along the southern coast of the gulf is reflected in Fig. 5 as a belt of saltier water extending to Tallinn Bay. The voluminous runoff of the Neva River leads to very low salinity in Neva Bay.

Comparison of the results for different model resolutions suggests that the use of a model with 0.5 NM resolution leads to a clear improvement of the quality of the simulations in two respects. First, the inflow of saltier water along the north-western coast of Estonia is represented by a continuous belt of saltier water while the 1 NM model hindcasts the presence of patches of saltier water. This difference is not unexpected: simulations in higher resolution are capable of reproducing the propagation of saltier water along a narrower nearshore area, for example, between the Island of Naissaar and the Estonian mainland. Second, the geometry of the salinity front at the entrance to Neva Bay is much more realistic for this particular wind situation. The model with a 0.5 NM resolution replicates the penetration of a tongue of saltier water into the southern part of this bay almost to the Island of Kotlin. There are also clear improvements in terms of the richness in detail in the patterns of sea surface temperature and currents when the resolution is increased from 1 to 0.5 NM (Fig. 7). This becomes especially evident in nearshore areas.

On the other hand, an increase in the model resolution from 0.5 to 0.25 NM adds much less to the resulting picture. Visually, only some changes of the features of saltier water inflow can be observed along the north-western coast of Estonia. The hydrophysical fields are, however, to some extent distorted by the presence of boundary and sponge layers in this area anyway. Therefore, the model with a resolution of 0.5 NM is apparently able to reproduce the majority of mesoscale features that affect the basin-scale redistribution of water masses. A further increase in the resolution is obviously necessary in order to properly

model small-scale features in the nearshore archipelago area of Finland and processes in the vicinity of the Island of Kotlin (Fig. 1) and the St. Petersburg Flood Protection Facility where the width of the gates is about 200 m. The further increase in resolution may also affect the stability properties of simulated coastal currents as discussed below.

Several features seen in Fig. 6 could shed some light on the problem of definition of the coastal zone for the North Estonian coast [51]. Namely, all model versions show a strong coastal jet along the north-eastern coast of Estonia that comes very close (to distance of about 2–3 km) to the coast. This current is separated from the coastal slope after passing the Kunda area and flows to the W–NW along the Lahemaa national park area. The separation occurs in the area where the relatively gently sloping nearshore of Narva Bay and Kunda Bay changes to an abruptly deepening section of the coast (Fig. 2). The latter geometry does not stabilize the flow along isobaths.

There is some controversy in the results of simulations with different resolutions as to what happens to this current in the central part of the gulf. The 1 and 0.5 NM simulations suggest that the coastal current continues along the Estonian coast through to the entrance to the gulf. On the contrary, the 0.25 NM simulation suggests that the current starts to meander and loses its identity. This scenario is predicted to occur quite frequently in simulations with a resolution of 2 NM [5]. Unfortunately, we have no *in situ* data to determine which scenario better reflects reality. This observation, however, confirms that the accuracy of representation of the nearshore and bottom geometry plays an important role in the behaviour of coastal currents in this basin and that an increase in the grid resolution down to 0.25 NM might be needed in order to properly reconstruct and forecast currents in some parts of the gulf.

An important (albeit not unexpected) consequence of this is that the complicated geometry of the coastal section at Lahemaa (where the sequence of several bays, deeply cut into mainland and peninsula stretching up to 15 km into the sea, dominate in the coastal geometry) effectively protects the nearshore (especially the bays) from the impact of the coastal current that may frequently exist along the southern coast of Narva Bay. This suggests that the dynamics of the nearshore waters is quite different for these two areas. One could expect very intense water exchange between the offshore and nearshore in Narva Bay and thus very limited ‘coastal’ dynamics in this section. On the contrary, the nearshore dynamics in the Lahemaa area is much more separated from offshore processes and the relevant nearshore area is apparently well defined [51].

5. SIMULATION OF TRAJECTORIES

The interaction of the high variability of the surface currents in the Baltic Sea [12,15,52] with the presence of fast current-driven transport in some sea areas [5,53] has initiated attempts to use the dynamics of the currents to develop

methods for the reduction of environmental risks. These attempts explore the potential for an increase in the time during which an adverse impact (for example, an oil spill) reaches a vulnerable area after an accident has happened. This increase may be achieved by locating the dangerous activities in sea areas (or redirecting ship traffic accordingly) so that the movement of the problem material to the coast is unlikely [54]. The first results indicate that transport patterns in some sea areas are essentially anisotropic so that the probability for a coastal section of being hit by an oil spill is not directly proportional to the distance from the pollution site [4].

The largest bottleneck in development of such methods is, as discussed above, the inability of deterministic circulation models to sensibly forecast the drift [3]. The trajectories of single drifters are highly sensitive with respect to the particular model and small variations of the initial and forcing conditions [2]. The problem is even more complicated in strongly stratified sea areas such as the Gulf of Finland where the drift is frequently steered by multi-layered dynamics [13]. For example, in 2003, GPS-positioned surface floating buoys were used to evaluate how well models can reproduce their drift in the Gulf of Finland. Model simulations, both in forecast and hindcast modes, were carried out by three 3D hydrodynamic models (HIROMB Seatrack Web [55,56], OpHespo model [57] and an earlier version of the OAAS model), the results of which were evaluated by comparing the calculated drifts with observations. These models were forced by HIRLAM (High Resolution Limited Area Model, run either by the Swedish Meteorological and Hydrological Institute or by the Finnish Meteorological Institute) and ECMWF (European Centre for Medium-Range Weather Forecasts) meteorological forecast fields.

In this study, the OAAS model covered the entire Baltic Sea area with a horizontal grid resolution of 2 NM. Although the model had 40 vertical layers in the Baltic Proper, the vertical resolution was quite coarse in the Gulf of Finland: the model has only 14 vertical layers, of which the surface layer was 2.5 m and the other layers 5–10 m thick. The simulated drift of the buoys, especially using the OAAS model, however, showed a good agreement with observations, even during a rapidly-changing wind situation when the winds turned about 100 degrees in half an hour over the investigation area [13]. Remarkably, the match of the simulated and measured drift was very good even in a few cases when some of the drifter positions were not recorded owing to technical problems and gradual correction of the modelled drifter positions was not possible. Therefore, the OAAS model adequately follows the drift of single floating objects in the surface layer of the Gulf of Finland during the first tens of hours after their release, provided the wind information is adequate.

There is, however, a multitude of relatively small-scale motions (frequently called sub-grid turbulence because it is not explicitly accounted for in the model) in the sea that generally tend to separate initially closely positioned drifters. This process of gradual separation is often called local turbulent spreading. The model should have a tool to simulate this process, otherwise all modelled particles

(virtual drifters [4]) released in a single grid cell will drift together for a long time, which is usually not the case in the ocean.

The effect of sub-grid turbulence is usually parameterized by means of slight perturbations of velocity components. Doing so generally results in local spreading of initially closely located particles. The relevant parameterization, however, should match the basic features of the flow regime in the area of interest. As shown by many numerical simulations and confirmed by recent ADCP measurements of currents [58], a most interesting feature of a substantial part of the motions in the Gulf of Finland with periods from 2 to 36 h is that they frequently are strongly circularly polarized. In other words, the direction of the flow changes quite rapidly and the flow mostly has an eddy-like structure rather than consisting of sections of unidirectional jet-like currents. This feature becomes even more dominant in high-resolution simulations (see above, Fig. 6) where high velocities are frequently connected with a strong rotation of the velocity vector. The frequent occurrence of such a motion regime where eddy rotation may dominate over unidirectional transport is not unexpected in the Gulf of Finland where the internal Rossby radius is very small. This feature is consistent with the peculiarity that the (directional) flow persistence is very low in the surface layer of the Gulf of Finland [12].

In order to account for this peculiarity of the current fields in the Gulf of Finland, we use an advanced modelling method for local turbulent spreading that accounts for the mostly rotational character of the currents in this basin. This feature can be, to a first approximation, accounted for by means of perturbing, say, the x component of velocity, based on the magnitude of the y component of velocity. We apply this concept by means of calculation of the displacement of the drifters from the following equations:

$$\frac{\mathrm{d}x}{\mathrm{d}t} = \hat{u} = u_c + crv, \quad \frac{\mathrm{d}y}{\mathrm{d}t} = \hat{v} = v_c + cru. \tag{9}$$

Here u_c and v_c are the modelled velocity components for this cell and $u' = crv$, $v' = cru$ are the local velocity perturbations defined with the use of random variable r that is uniformly distributed within the interval [–0.5, 0.5]. The advantage of doing this is twofold. Firstly, this method tends to conserve the high speeds of the drifter. Secondly, it mimics the strong rotational component of the motion and thus works as an analogue of the Coriolis force with random amplitude but with no directional preference. For example, if a particle is moving rapidly in the x direction, it has a high chance of deviating from this direction because v' is proportional to u whereas its speed is more or less maintained because there will be no changes to u. Equations (9) are solved with the use of the Euler method

$$x^{n+1} = x^n + \Delta t\hat{u}, \quad y^{n+1} = y^n + \Delta t\hat{v}. \tag{10}$$

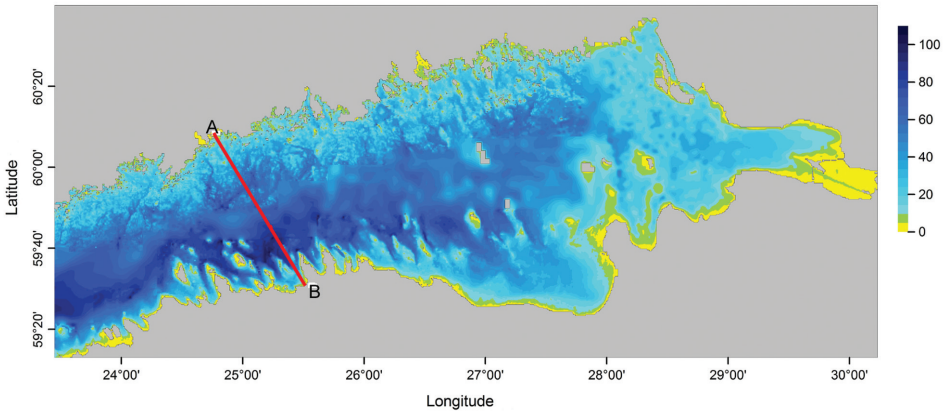

Fig. 2. Water depths (m) in the Gulf of Finland with a spatial resolution of 0.25 NM along the coasts of Estonia and Finland and about 0.5 NM in the eastern part of the gulf and in the area between Finland and Estonia not covered by high-resolution navigation maps.

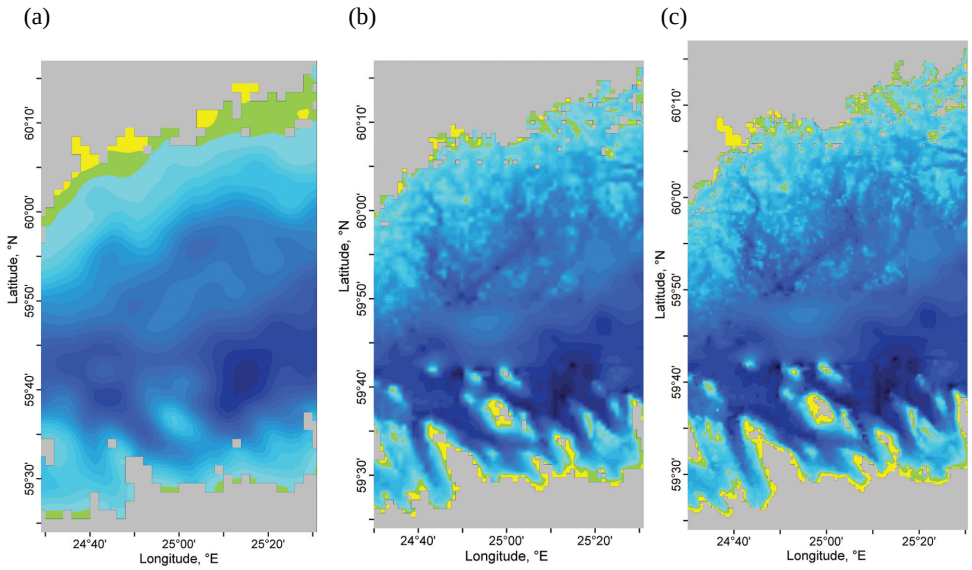

Fig. 3. The bathymetry of the sea area between Tallinn and Helsinki in three resolutions: (a) 1 NM [14]; (b) 0.5 NM; (c) 0.25 NM. Colour scale is the same as for Fig. 2.

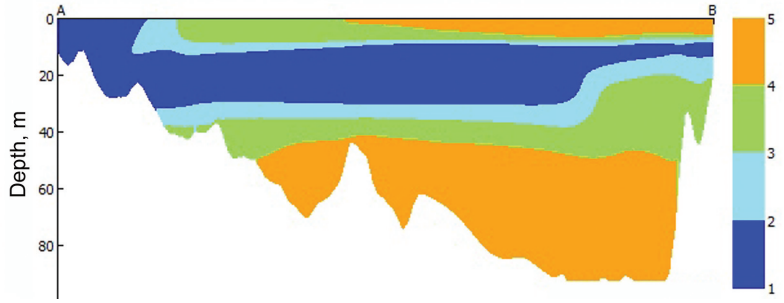

Fig. 4. Cross-section of water temperature (indicated in °C) along the line A–B (Fig. 6c) on 16 May 1996 at 22:00 GMT.

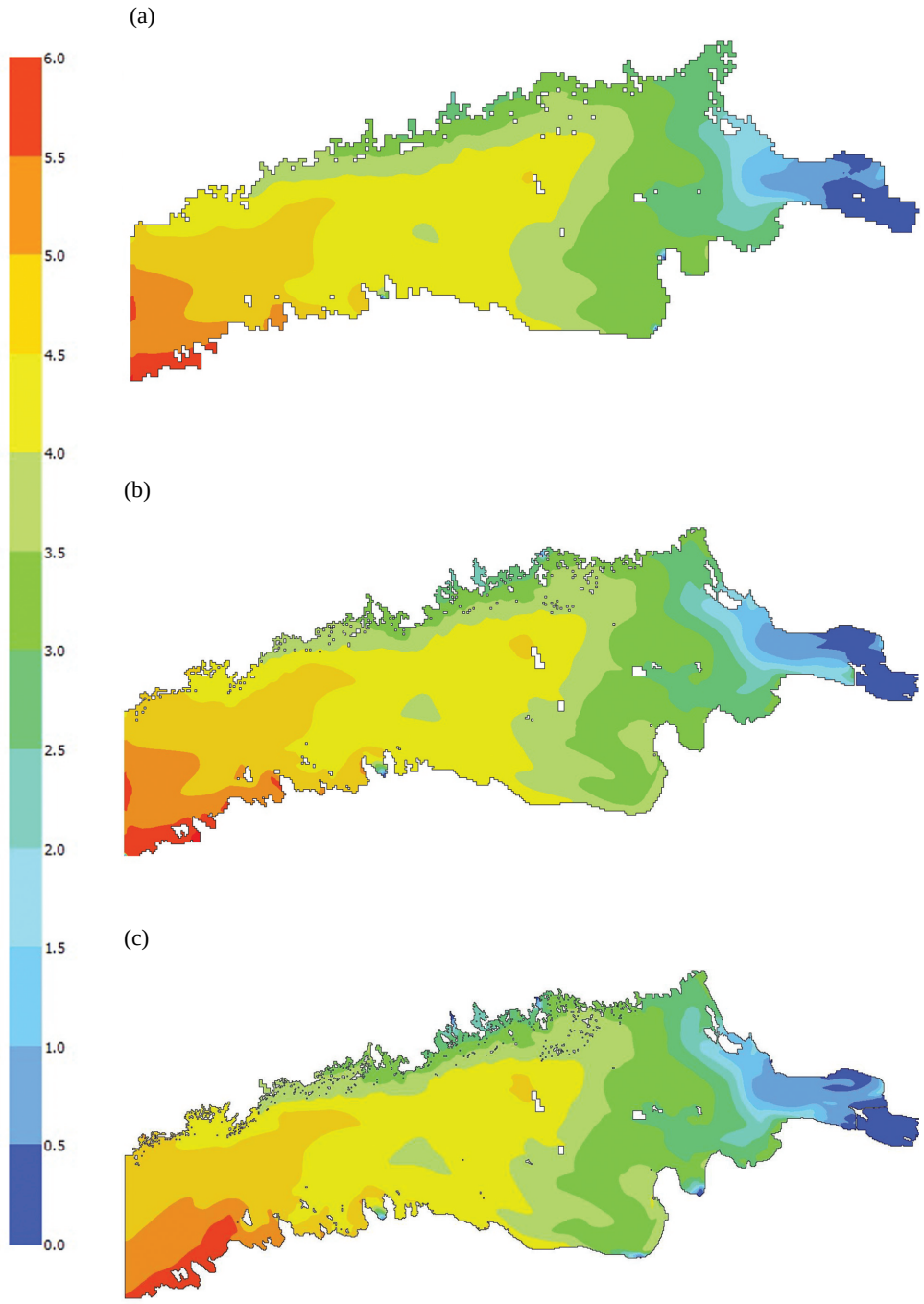

Fig. 5. Spatial distribution of surface salinity (‰) in the Gulf of Finland on 16 May 1996 at 22:00 GMT calculated with a resolution of 1 NM (a), 0.5 NM (b), and 0.25 NM (c).

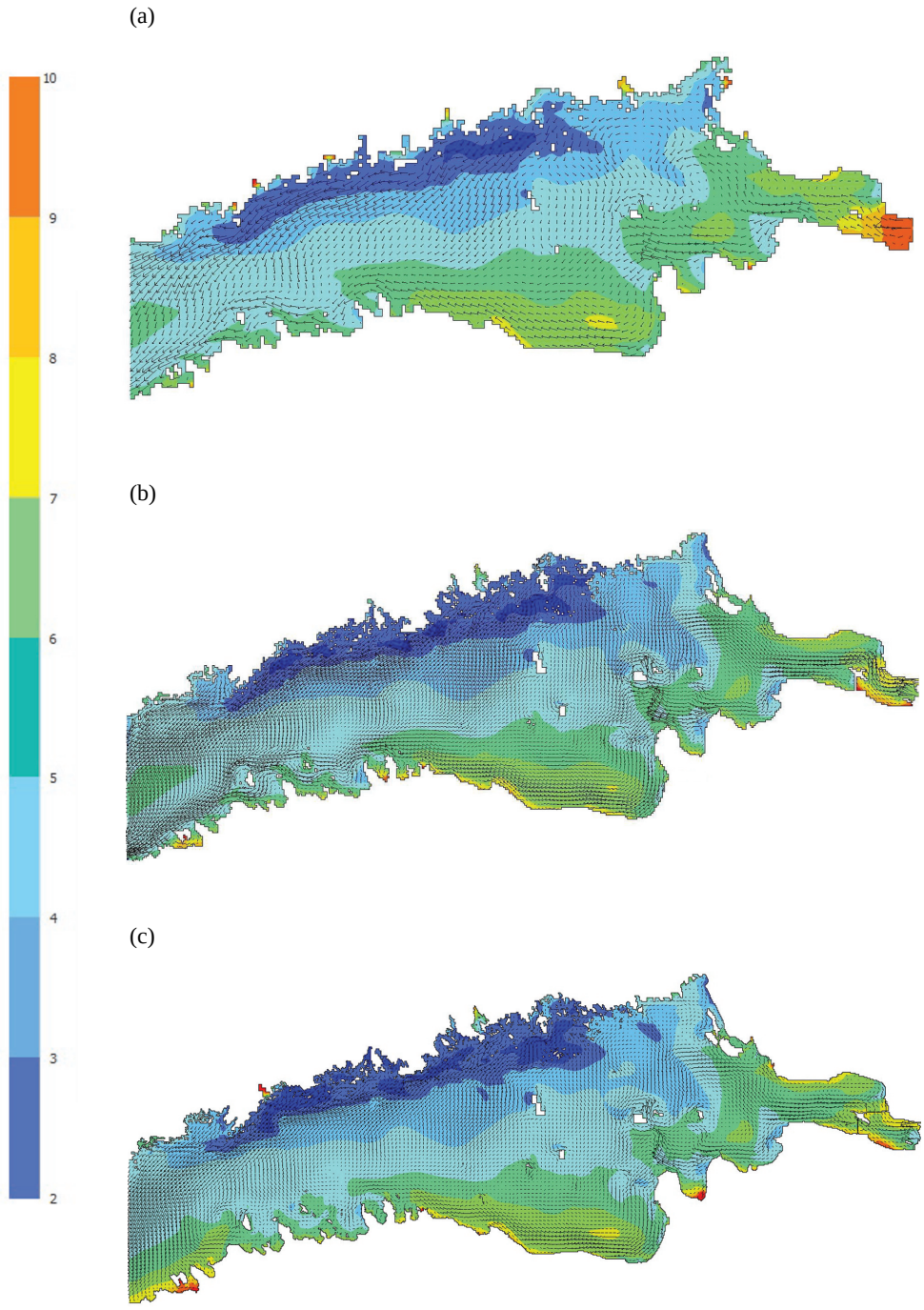

Fig. 6. Velocities (vectors) and sea surface temperatures (colour scale) in the Gulf of Finland on 16 May 1996 at 22:00 GMT calculated with a resolution of 1 NM (a), 0.5 NM (b), and 0.25 NM (c).

(a)

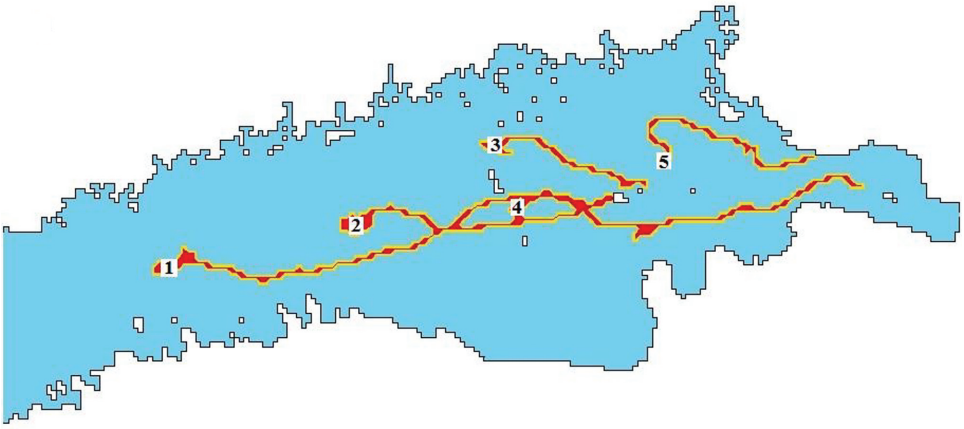

(b)

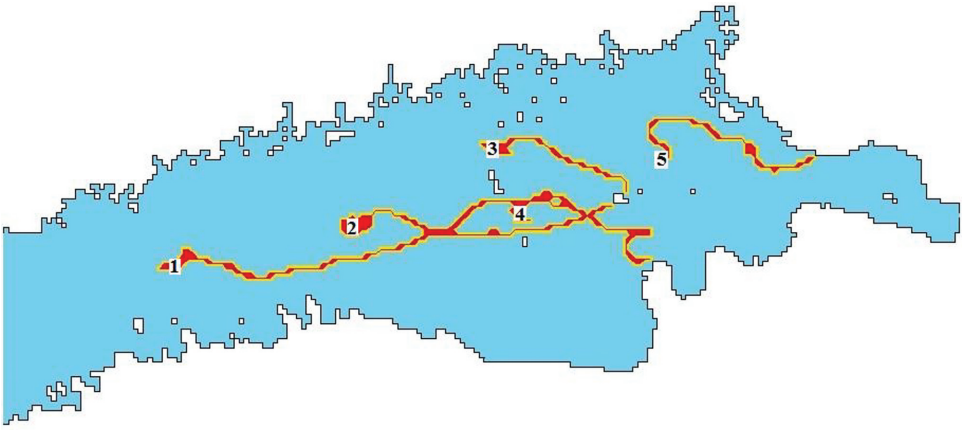

Fig. 7. Examples of trajectories of pairs of particles released into five grid cells in the Gulf of Finland in January 1990.

The integration time step in Eqs. (10) is equal to the time step of the circulation model (Table 1). Given the maximum surface velocities in the order of 1 m/s, the maximum displacement of particles within one time step is 180 m in simulations with the resolution of 1 NM, which is much less than the grid cell size. The typical displacement is of course much smaller, usually a few tens of metres. The magnitude of the described effect of local turbulence is defined by the coefficient c. It has been set to 1 in the current experiments (that is, the maximum effect to the velocity is 50% from its instantaneous value). This value may need further tuning based on physical experiments that are in progress.

Differently from the off-line method of calculation of trajectories, implemented in the TRACMASS code [59–61] and in the relevant studies where velocity fields are updated once in a few hours [4,5], our calculations are performed simultaneously with the runs of the circulation model. Doing so allows for much more exact reproduction of single trajectories. As the local velocity fields carrying the drifters are updated after each time step, even the use of the simplest, linear approximation of the trajectories within each time step and the Euler method to solve systems of differential equations for the trajectories leads to very good results as demonstrated in [13].

A few realizations of the resulting trajectories in the surface layer are presented in Fig. 7. The influence of the random fluctuations created is in general fairly small, and the trajectories typically remain quite close to each other. This feature suggests that the proposed spreading scheme qualitatively matches the largely rotational character of the mesoscale dynamics in the sense that the particles with perturbed velocities still follow the local eddy rotation. There are, however, cases (for example, particle 4 in Fig. 7) when initially close particles follow completely different flow paths and are carried to a distance of many tens of km from each other. The proportion of such cases apparently reflects the probability of occurrence of highly divergent areas of the surface flow, for example, areas where mesoscale eddies come close to each other.

The mean final distance for a set of $N = 17\,620$ pairs of particles (Table 1, two particles inserted into each sea grid cell of a 1 NM model) for the period from December 1990 to November 1991, averaged over time windows with duration of 10 days, shows substantial seasonal variability (Fig. 8). The average final distance is usually the largest (up to about 5 km, that is, more than 10 grid cells) during the windiest months (October–December) although there are some time windows with quite limited increase in the distance during these months. The typical separation reached within the time windows in question is in the range of 1–2 km (2–4 grid cells). The overall average separation rate is about 176 m/day or 2 mm/s, which is about 8% of the overall average surface-layer speed [5]. This estimate is realistic for the dynamics of the Gulf of Finland where the high variability of forcing and the current patterns evidently gives rise to relatively large levels of small-scale turbulence. However, for practical applications the coefficient c, characterizing the modelled spreading, should be calibrated with *in situ* measurements.

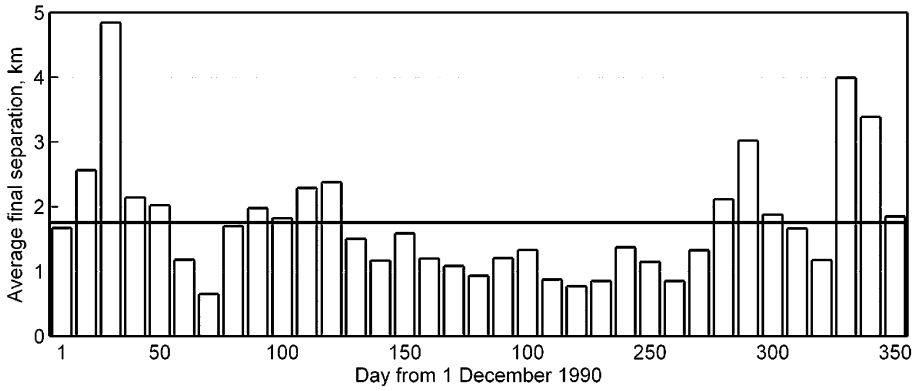

Fig. 8. The average final distance after 10 days of propagation of initially closely located particles in the Gulf of Finland. The horizontal scale indicates the initial day of propagation starting from 1 December 1990. The horizontal line shows the overall average over all time windows.

6. DISCUSSION

We have extended attempts to reduce the uncertainties of the current-induced drift patterns, identified by means of statistical analysis of large pools of numerically simulated Lagrangian trajectories in the Gulf of Finland [4], in two important aspects. Firstly, we have implemented a new set of bathymetric information with a spatial resolution of 0.25 NM (about 470 m) in the nearshore of Finland and Estonia. For areas for which such detailed information is not available (mostly the deepest areas and the regions in the east of the gulf), gridded bathymetry with a resolution of 0.5 NM has been used. Based on this data set, we have upgraded the 3D circulation model OAAS (that is specifically fine-tuned for the hydrographic conditions of the Gulf of Finland) to better resolve the details of the current fields in the Gulf of Finland.

An increase in the spatial resolution for circulation modelling in this basin to about 0.5 NM is essential for adequate simulations of the statistics of current patterns in this basin while systematically accounting for most mesoscale effects. The increase in horizontal resolution is accompanied by an enhanced vertical resolution of the model that now uses up to 105 vertical levels. Preliminary experiments with this resolution are most promising. The spatial patterns of surface currents and temperatures show highly detailed patterns that qualitatively match well with the expected features. The need for further improvement of the horizontal model resolution is not obvious and should be established based on systematic comparison of the modelled and measured data.

Secondly, these improvements of the model and its resolution permit further extensions of its application, especially in terms of its potential to account for the effects of sub-grid-scale turbulence upon the drift of clusters of floating objects. In order to accomplish this task, we have introduced a new method of parameterization of sub-grid turbulence that accounts for the highly rotational

character of the Gulf of Finland current fields. This way of parameterization is necessary in this basin where the typical turnover time of mesoscale eddies is a few days and where eddy rotation frequently dominates in the flow patterns. The parameter describing the magnitude of its effect should be estimated from *in situ* measurements of spreading of drifters that are currently in the planning stage.

ACKNOWLEDGEMENTS

This study was performed in the framework of the BONUS+ project BalticWay (financed by the BONUS EEIG). This initiative attempts to identify the regions in the Baltic Sea that are associated with increased risk compared to other sea areas and to propose ways to reduce the risk of them being polluted by placing activities in other areas. The research was also partially supported by the Marie Curie Reintegration Grant ESTSpline (PERG02-GA-2007-224819), targeted financing by the Estonian Ministry of Education and Research (grant SF0140077s08) and the Estonian Science Foundation (grant No. 7413). The authors sincerely thank Kai Myrberg and Vladimir Ryabchenko for their comments and suggestions.

REFERENCES

1. Myrberg, K., Ryabchenko, V., Isaev, A., Vankevich, R., Andrejev, O., Bendtsen, J., Erichsen, A., Funkquist, L., Inkala, A., Neelov, I. et al. Validation of three-dimensional hydrodynamic models in the Gulf of Finland based on a statistical analysis of a six-model ensemble. *Boreal Env. Res.*, 2010, **15**. Forthcoming.
2. Griffa, A., Piterbarg, L. I. and Ozgokmen, T. Predictability of Lagrangian particle trajectories: effects of smoothing of the underlying Eulerian flow. *J. Marine Res.*, 2004, **62**, 1–35.
3. Vandenbulcke, L., Beckers, J.-M., Lenartz, F., Barth, A., Poulain, P.-M., Aidonidis, M., Meyrat, J., Ardhuin, F., Tonani, M., Fratianni, C. et al. Super-ensemble techniques: Application to surface drift prediction. *Progr. Oceanogr.*, 2009, **82**, 149–167.
4. Soomere, T., Viikmäe, B., Delpeche, N. and Myrberg, K. Towards identification of areas of reduced risk in the Gulf of Finland, the Baltic Sea. *Proc. Estonian Acad. Sci.*, 2010, **59**, 156–165.
5. Soomere, T., Delpeche, N., Viikmäe, B., Quak, E., Meier, H. E. M. and Döös, K. Patterns of current-induced transport in the surface layer of the Gulf of Finland. *Boreal Env. Res.*, 2011, **16**. Forthcoming.
6. Drijfhout, S. S. Eddy-genesis and the related heat transport: A parameter study. In *Mesoscale/Synoptic Coherent Structures in Geophysical Turbulence* (Nihoul, J. C. J. and Jamart, B. M., eds.). Elsevier Oceanography Series, 1989, **50**, 245–263.
7. Lindow, H. *Experimentelle Simulationen windangeregter dynamischer Muster in hochauflösenden numerischen Modellen*. Meereswissenschaftliche Berichte No. 22. Institut für Ostseeforschung, Warnemünde, 1997.
8. Meier, H. E. M., Döscher, R. and Faxén, T. A multiprocessor coupled ice-ocean model for the Baltic Sea: Application to salt inflow. *J. Geophys. Res.*, 2003, **108**, C3273.
9. Meier, H. E. M. Modeling the pathways and ages of inflowing salt- and freshwater in the Baltic Sea. *Estuar. Coast. Shelf Sci.*, 2007, **74**, 717–734.

10. Alenius, P., Nekrasov, A. and Myrberg, K. The baroclinic Rossby-radius in the Gulf of Finland. *Cont. Shelf Res.*, 2003, **23**, 563–573.
11. Leppäranta, M. and Myrberg, K. *Physical Oceanography of the Baltic Sea*. Springer Praxis, 2009.
12. Andrejev, O., Myrberg, K., Alenius, P. and Lundberg, P. A. Mean circulation and water exchange in the Gulf of Finland – a study based on three-dimensional modelling. *Boreal Env. Res.*, 2004, **9**, 1–16.
13. Gästgifvars, M., Lauri, H., Sarkanen, A.-K., Myrberg, K., Andrejev, O. and Ambjörn, C. Modelling surface drifting of buoys during a rapidly-moving weather front in the Gulf of Finland, Baltic Sea. *Estuar. Coast. Shelf Sci.*, 2006, **70**, 567–576.
14. Seifert, T., Tauber, F. and Kayser, B. A high resolution spherical grid topography of the Baltic Sea. In *Proc. Baltic Sea Science Congress*. Stockholm, 2001, vol. 2, Poster # 147, www.io-warnemuende.de/iowtopo
15. Andrejev, O., Myrberg, K. and Lundberg, P. A. Age and renewal time of water masses in a semi-enclosed basin – Application to the Gulf of Finland. *Tellus*, 2004, **56A**, 548–558.
16. Soomere, T. Anisotropy of wind and wave regimes in the Baltic Proper. *J. Sea Res.*, 2003, **49**, 305–316.
17. Soomere, T. Wind wave statistics in Tallinn Bay. *Boreal Env. Res.*, 2005, **10**, 103–118.
18. Passenko, J., Lessin, G., Erichsen, A. C. and Raudsepp, U. Validation of hydrostatic and non-hydrostatic versions of hydrodynamical model MIKE 3 applied for the Baltic Sea. *Estonian J. Eng.*, 2008, **14**, 255–270.
19. Zhurbas, V., Laanemets, J. and Vahtera, E. Modeling of the mesoscale structure of coupled upwelling/downwelling events and the related input of nutrients to the upper mixed layer in the Gulf of Finland, Baltic Sea. *J. Geophys. Res.*, 2008, **113**, C05004.
20. Zhurbas, V. M., Laanemets, J., Kuzmina, N. P., Muraviev, S. S. and Elken, J. Direct estimates of the lateral eddy diffusivity in the Gulf of Finland of the Baltic Sea (based on the results of numerical experiments with an eddy resolving model). *Oceanology*, 2008, **48**, 175–181.
21. Lips, U., Lips, I., Liblik, T. and Elken, J. Estuarine transport versus vertical movement and mixing of water masses in the Gulf of Finland (Baltic Sea). In *IEEE/OES US/EU-Baltic International Symposium*. Tallinn, Estonia, 2008. IEEE, 2008, 326–333.
22. Laanemets, J., Zhurbas, V., Elken, J. and Vahtera, E. Dependence of upwelling-mediated nutrient transport on wind forcing, bottom topography and stratification in the Gulf of Finland: model experiments. *Boreal Env. Res.*, 2009, **14**, 213–225.
23. Seifert, T. and Kayser, B. A high resolution spherical grid topography of the Baltic Sea. Meereswissenschaftliche Berichte 9, Institut für Ostseeforschung, Warnemünde, 1995.
24. Elken, J. Modelling of coastal circulation and oil drift at possible deep harbour sites, north-western Saaremaa Island. *Proc. Estonian Acad. Sci. Eng.*, 2001, **7**, 141–156.
25. Suursaar, Ü., Kullas, T. and Otsmann, M. Hydrodynamic modelling of sea levels in the Väina-meri and Pärnu Bay. *Proc. Estonian Acad. Sci. Eng.*, 2001, **7**, 222–234.
26. Laanearu, J., Koppel, T., Soomere, T. and Davies, P. A. Joint influence of river stream, water level and wind waves on the height of sand bar in a river mouth. *Nord. Hydrol.*, 2007, **38**, 287–302.
27. Torsvik, T. and Soomere, T. Modeling of long waves from high speed ferries in coastal waters. *J. Coastal Res.*, 2009, SI **56**, vol. II, 1075–1079.
28. Torsvik, T., Didenkulova, I., Soomere, T. and Parnell, K. E. Variability in spatial patterns of long nonlinear waves from fast ferries in Tallinn Bay. *Nonlin. Processes Geophys.*, 2009, **16**, 351–363.
29. Averkiev, A. S. and Klevanny, K. A. Determining cyclone trajectories and velocities leading to extreme sea level rises in the Gulf of Finland. *Meteorol. Hydrol.*, 2007, **8**, 55–63 (in Russian).
30. Ryabchenko, V., Dvornikov, A., Haapala, J. and Myrberg, K. Modelling ice conditions in the easternmost Gulf of Finland in the Baltic Sea. *Cont. Shelf Res.*, 2010, **30**, 1458–1471.
31. Andrejev, O. and Sokolov, A. Numerical modelling of the water dynamics and passive pollutant transport in the Neva inlet. *Meteorol. Hydrol.*, 1989, **12**, 75–85 (in Russian).

32. Andrejev, O. and Sokolov, A. 3D baroclinic hydrodynamic model and its applications to Skagerrak circulation modelling. In *Proc. 17th Conference of the Baltic Oceanographers.* Norrköping, Sweden, 1990, 38–46.
33. Bryan, K. A numerical method for the study of the circulation of the World Ocean. *J. Comp. Phys.*, 1969, **4**, 347–376.
34. Smagorinsky, J. General circulation experiments with the primitive equations, I. The basic experiment. *Mon. Weather Rev.*, 1963, **91**, 99–164.
35. Kochergin, V. P. Three-dimensional prognostic models. In *Three-dimensional Coastal Ocean Models* (Heaps, N. S., ed.), Am. Geophys. Union, *Coast. Estuar. Sci. Ser.*, 1987, **4**, 201–208.
36. Millero, F. and Kremling, I. The densities of the Baltic Sea deep waters. *Deep Sea Res.*, 1976, **23**, 1129–1138.
37. Niiler, P. and Kraus, E. One-dimensional models of the upper ocean. In *Modelling and Prediction of the Upper Layers of the Ocean* (Kraus, E., ed.). Pergamon Press, Oxford, 1977, 143–172.
38. Bunker, J. Computations of surface energy flux and annual air-sea interaction cycle of the North Atlantic. *Mon. Weath. Rev.*, 1977, **105**, 33–65.
39. Blumberg, A. and Mellor, G. A description of a three-dimensional coastal ocean circulation model. In *Three-dimensional Coastal Ocean Models* (Heaps, N. S., ed.). American Geophys. Union, *Coast. Estuar. Sci. Ser.*, 1987, **4**, 1–16.
40. Proudman, J. *Dynamical Oceanography*. Methuen & Co., London, 1953.
41. Sokolov, A., Andrejev, O., Wulff, F. and Rodriguez Medina, M. *The Data Assimilation System for Data Analysis in the Baltic Sea*. *System Ecology Contributions*, No. 3. Stockholm University, Sweden, 1997.
42. Mesinger, F. and Arakawa, A. Numerical methods used in atmospheric models. *GARP Publ. Ser.*, No. 17, I, 1976.
43. Liu, S.-K. and Leendertse, J. Multidimensional numerical modelling of estuaries and coastal seas. *Adv Hydrosci.*, 1978, **11**, 95–164.
44. Simons, T. J. Verification of numerical models of Lake Ontario. Part I. Circulation in spring and early summer. *J. Phys. Oceanogr.*, 1974, **4**, 507–523.
45. Orlanski, I. A simple boundary condition for unbounded hyperbolic flows. *J. Comp. Phys.*, 1976, **21**, 251–269.
46. Mutzke, A. Open boundary condition in the GFDL-model with free surface. *Ocean Model.*, 1998, **116**, 2–6.
47. Höglund, A., Meier, H. E. M., Broman, B. and Kriezi, E. *Validation and Correction of Regionalised ERA-40 Wind Fields over the Baltic Sea Using the Rossby Centre Atmosphere Model RCA3.0*. Rapport Oceanografi No. 97, Swedish Meteorological and Hydrological Institute, SE-60176. Norrköping, Sweden, 2009.
48. Bergström, S. and Carlsson, B. River runoff to the Baltic Sea: 1950–1990. *Ambio*, 1994, **23**, 280–287.
49. Myrberg, K. and Andrejev, O. Main upwelling regions in the Baltic Sea – a statistical analysis based on three-dimensional modelling. *Boreal Env. Res.*, 2003, **8**, 97–112.
50. Soomere, T., Myrberg, K., Leppäranta, M. and Nekrasov, A. The progress in knowledge of physical oceanography of the Gulf of Finland: a review for 1997–2007. *Oceanologia*, 2008, **50**, 287–362.
51. Lessin, G., Ossipova, V., Lips, I. and Raudsepp, U. Identification of the coastal zone of the central and eastern Gulf of Finland by numerical modeling, measurements, and remote sensing of chlorophyll *a*. *Hydrobiologia*, 2009, **692**, 187–198.
52. Lehmann, A., Krauss, W. and Hinrichsen, H.-H. Effects of remote and local atmospheric forcing on circulation and upwelling in the Baltic Sea. *Tellus*, 2002, **54A**, 299–316.
53. Osinski, R. and Piechura, J. Latest findings about circulation of upper layer in the Baltic Proper. In *BSSC 2009 Abstract Book*. Tallinn, Estonia, 2009, 103.
54. Soomere, T. and Quak, E. On the potential of reducing coastal pollution by a proper choice of the fairway. *J. Coastal Res.*, 2007, SI **50**, 678–682.

55. Funkquist, L. HIROMB, an operational eddy-resolving model for the Baltic Sea. *Bulletin of the Maritime Institute*. Gdańsk, 2001, No. 28, 7–16.
56. Gästgifvars, M., Ambjörn, C. and Funkquist, L. Operational modelling of the trajectory and fate of spills in the Baltic Sea. In *Proc. 25th Arctic and Marine Oil-spill Program (AMOP) Technical Seminar*. Calgary, Canada, 2001. Environment Canada, 2002, 1115–1130.
57. Korpinen, P., Kiirikki, M., Koponen, J., Peltoniemi, H. and Sarkkula, J. Evaluation and control of eutrophication in Helsinki sea area with the help of a nested 3D-ecohydrodynamic model. *J. Marine Syst.*, 2004, **45**, 255–265.
58. Lilover, M.-J., Pavelson, J. and Kõuts, T. Wind forced currents over shallow Naissaar Bank in the Gulf of Finland. *Boreal Env. Res.*, 2011, **16**. Forthcoming.
59. Döös, K. Inter-ocean exchange of water masses. *J. Geophys. Res.*, 1995, **100**, C13499–C13514.
60. de Vries, P. and Döös, K. Calculating Lagrangian trajectories using time-dependent velocity fields. *J. Atmos. Oceanic Technol.*, 2001, **18**, 1092–1101.
61. Engqvist, A., Döös, K. and Andrejev, O. Modeling water exchange and contaminant transport through a Baltic coastal region. *Ambio*, 2006, **35**, 435–447.

Kõrglahutusega batümeetria Soome lahe hüdrodünaamika mudelis

Oleg Andrejev, Alexander Sokolov, Tarmo Soomere,
Rolf Värv ja Bert Viikmäe

Soome lahe hüdrodünaamika numbrilise mudeli OAAS lahutusvõimet on digiteeritud merekaartide alusel koostatud batümeetrilise info baasil, suurendatud 0,25 meremiilini horisontaalsuunas ja 1 meetrini vertikaalsuunas. Ühemiilise ja parema lahutusvõimega mudelid peegeldavad adekvaatselt mesomastaapsete keeriste süsteeme sellel merealal, kus barokliinne Rossby raadius on enamasti 2–4 km. Mudeli lahutusvõime suurendamine 0,5 miilini võimaldab ühemiilise sammuga mudeliga võrreldes märksa detailsemalt rekonstrueerida kesksete hüdrofüüsikaliste väljade (näiteks temperatuur ja soolsus) omadusi. Lahutusvõime edasise suurendamisega 0,25 miilini lisandub suhteliselt vähem temperatuuri ja soolsuse detaile, kuid hoovuste mustrites võivad ilmneda suhteliselt suured erinevused. On esitatud uus meetod, parametriseerimaks pinnakihis algselt üksteise lähedal paiknevate objektide vahelise kauguse muutusi kohaliku turbulentsi mõjul, mis arvestab Soome lahe hoovuste eripära – suhteliselt kiireid hoovuste suuna muutusi. On näidatud, et 1991. aasta hüdrodünaamilistes tingimustes kaugenesid objektid üksteisest kiirusega ligikaudu 2 mm/s.